

# Emulating a Sensor for the Measurements of the Hydraulic Resistances of Nozzles in Agricultural Sprayers Based on the Use of the Point-Wise Thévenin's Theorem

Rafael F. Q. Magossi<sup>1,2</sup>, Elmer A. G. Peñaloza<sup>1,2</sup>, Shankar P. Battacharya<sup>3</sup>,  
 Vilma A. Oliveira<sup>2</sup>, Paulo E. Cruvinel<sup>1</sup>

<sup>1</sup>Embrapa Instrumentation  
 Brazilian Agricultural Research Corporation, São Carlos, SP, Brazil  
 Email: paulo.cruvinel@embrapa.br

<sup>2</sup> Department of Electrical and Computer Engineering  
 University of São Paulo, São Carlos, SP, Brazil  
 Email: rafael.magossi, egamboa, voliveira@usp.br

<sup>3</sup>Department of Electrical and Computer Engineering  
 Texas A&M University, College Station, Texas, USA  
 Email: bhatt@ece.tamu.edu

**Abstract**—In agriculture, the chemicals should be applied evenly and at a prescribed rate. An accurately calibrated boom will ensure that this is achieved. In addition, the correct use of pesticides can deliver significant environmental and socio-economic benefits in the form of safe, healthy, and affordable food, as well as to decrease the impact in natural resources such as soil, water and overall land use. The quality of pesticides application is dependent on the hydraulic fluidic resistance present in the nozzles of the sprayers. This paper presents a method to evaluate the hydraulic pressure drop in bars of agricultural sprayer systems using the fluid hydraulic resistance as a part of a sensor element associated with point-wise Thévenin's equivalents. This method makes it possible to control and measure the pressure drop at lower cost and greater accuracy. In this context, taking into account a measurement-based approach, a parameterized relationship among operating conditions and the fluidic resistance was defined. Therefore, it was possible to obtain the hydraulic equivalents of a sprayer system with direct injection based only on the hydraulic flow and pressure measurements. The results have shown that it is possible to obtain the hydraulic equivalent resistances with a relative error equal to 2.15%. Furthermore, the relationship among the orifice nozzle diameter, pressure and flow was also found.

**Keywords**—Measurement theory; Parameterized model; Point-wise Thévenin's equivalent; Electrical-hydraulic analogy; Agricultural quality sensor; Food safety; Risk analysis.

## I. INTRODUCTION

Nowadays, hydraulic systems can be found in a wide variety of applications, including agriculture. For such systems it is important to determine the internal losses occurring not only for the set up of upstream and downstream pressure valves, but also to calculate the flow rates through piping systems. In this context, the fluid hydraulic resistance from the nozzles used in the agricultural sprayers plays an important role. A previous discussion related to such content was presented in [1]. In addition, such information can assist in establishing the flow rate range associated with pumps, compressors, turbines, and relief headers to ensure that back pressure on the relief devices does not prevent them from functioning properly [2].

Pesticide application is a vital component for food security, and production is directly connected to pest control. Agricultural sprayers are used to apply liquid chemicals on plants to control pests and diseases. In addition, it can be used to apply herbicides to control weeds and to apply fertilizers to enhance plants growth. There are many types of sprayers commercially available to producers designed for their own specific functions and use. One may find backpack sprayers, hand compression sprayers, self-propelled sprayers, aerial sprayers, and pull-behind sprayers, among others.

The manual application method was the first to be used in agriculture, but it has the disadvantage that it presents a higher risk to humans. On the other hand, turning off sprayers when there is no target, or adjusting application rates based on canopy size and density became essential for production with sustainability, that is, in such matters the automated sprayers play an important role. Close to the 90's, manufacturers introduced precision spraying technology in boom sprayers [3]. Despite being still an open field for research and innovation, the variable rate methods, using the Global Position System (GPS) and the Geographic Information System (GIS) technologies were integrated into boom sprayers and became already commercially available.

The adoption of precision agriculture (PA) for localized application of agrochemicals can reduce pesticide wastage and environmental aggression, providing a more efficient production of large-scale food and increasing agricultural productivity. With localized application of agrochemicals, herbicide savings is in the order of 30 to 80% compared to the uniform application in the total area. Automatic sprayers designed and developed for localized application are currently available, allowing the use of large volume of syrup, covering large agricultural areas [4]–[7].

In this field of knowledge, there are the use of conventional and direct injection sprayer systems. The first type of direct injection system was developed between the 70's and 80's. However, in that time such a system presented high cost, complexity of operation and low performance. According to

Baio and Antuniassi [6], the main characteristic of direct injection systems is related to the storage of the diluent (water) and pesticide in separate containers.

The mixing of pesticides and water is carried out only at the time of application, by injection of the pesticide into the piping, which carries the syrup to the nozzles of the sprayer. The amount of injected pesticide can be accomplished, among other ways, by controlling the rotation of the piston or peristaltic injection pumps. The main advantages of the injection system are the reduction of risks involved during the application process [8].

Other aspects one should take into account, in relation to this matter, is the benefit/cost rate in terms of the use of energy in the agricultural machinery. Most fluid energy systems are configured with a positive flow displacement pump that is large enough to meet the flow requirements of many circuits. Different work functions require a variety of flow and pressure values to provide the desired operation. Branches of the system therefore must include specific flow and pressure regulating valves.

This paper presents a method based on a measurement approach to evaluate the hydraulic pressure drop in booms of agricultural sprayer systems using the fluid hydraulic resistance as part of a sensor element associated with a point-wise Thévenin's equivalent measurement method.

The next sections of the paper are organized as follows. In Section II the concepts of spraying quality and fluidic resistance are given. In Section III, the theoretical background for the understanding of the parameterized input-output model and the theoretical development of the measurement based approach for unknown systems and the analog models between the electrical and hydraulic circuits to obtain point-wise hydraulic Thévenin's equivalent are studied. Subsequently, in Section IV, the method used to obtain the internal loss, pressure equivalents and the function relating the nozzle orifice diameter and pressure with the flow in a full cone nozzle is given. In Section V, the experimental validation of both the nozzle flow in terms of operating conditions and the point-wise Thévenin's equivalents using a laboratory sprayer setup are performed. Finally, some concluding remarks are presented in Section VI.

## II. AGRICULTURAL SPRAYING QUALITY

As the fluid moves inside a pipe occur a turbulence of the fluid with itself and a fluid friction with the inner walls of this pipe. This causes the pressure inside the pipe to gradually decrease as the fluid moves. The pressure decrease is known as the pressure drop. In this way, the load loss would be related to a resistance to the passage of the flow of the fluid inside the pipe. This resistance is known as fluidic resistance and directly affects the volumetric flow [9], [10]. Moreover, the fluid hydraulic resistance is subject to temporal variations requiring a considerable effort to be determined. In Figure 1 it can be observed the functioning of a full cone nozzle and the characterization of a fluidic resistance.

In the process of agricultural spraying, it is of great importance to know the value of the fluidic resistance of the spray boom since variations in this resistance can affect the quality of the application, that is, size and volume of drops, distribution of drops on the crop and the drift of the drops produced by the wind [11].

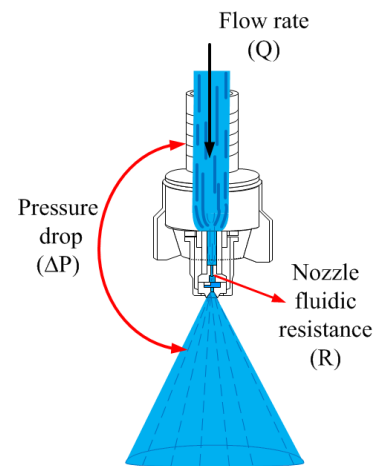


Figure 1. Representation of a hydraulic full cone nozzle where for a given flow rate there is a pressure drop caused by the fluidic resistance, which is related to the internal mechanical characteristics of this nozzle.

Therefore, the value of the fluidic resistance as well as its behavior as a function of the operating conditions yield relevant information to infer the quality of the pesticides application. Droplet size and its distribution are critical factors in such processes because can affect the penetration, coverage and drift of the application on the crop [12].

The design of a hydraulic system can be improved with the use of mathematical simulation. Numerous approaches to energy systems modeling fluids and components can be found in the literature. Analysis of a fluid feed system can cover the flow distribution, the functioning of components, or a combination of both. Most of the useful equations for fluid analysis are derived from the law of conservation of energy, the principle of continuity, and Newton's second law [13].

Equations used to calculate flow in circuits involve the use of empirical expressions or laboratory-derived flow coefficients. Therefore, when two or more circuits are used simultaneously, the principle of continuity may not be obeyed exactly, because of the use of such empirical coefficients.

To determine the desired pressure and flow values, a set of equations can be solved via an iterative method. Iterative methods work well under steady state flow conditions. However, they are difficult to apply under non-steady state operations. In relation to this subject Akers and collaborators proposed a method based on electrical-hydraulic analogy [9]. In such method, the fluid pressure, the flow, and the fluidic resistance are analogous to voltage, current, and electrical resistance, respectively. The method uses the basic principle of Ohm's law, also referred to as the hydraulic Ohm.

In this scenario, a sensor that can measure the internal losses of the hydraulic boom in sprayers is very much required. The boom pressure drop denoted  $\Delta P$  can be related to the volumetric flow rate denoted  $Q$  by:

$$\Delta P = f_a \frac{L\rho}{2DA^2} Q^2 \quad (1)$$

for a rough pipe with turbulent flow or:

$$\Delta P = \frac{8\pi L\mu}{A^2} Q^2 \quad (2)$$

for a flat tube with laminar flow, where  $f_a$  is the coefficient of friction [dimensionless],  $\rho$  is the specific mass of the fluid [ $kg/m^3$ ],  $L$  is the equivalent pipe length [ $m$ ],  $D$  is the internal diameter of the pipe [ $m$ ],  $A$  is the inner area of the straight section of the pipe [ $m^2$ ] and  $\mu$  is the absolute viscosity of the fluid [ $P_a \cdot s$ ].

The coefficient of friction  $f_a$ , sometimes known as a Moody friction factor or also as a distributed load loss coefficient determined by mathematical equations, is a function of the Reynolds number and relative roughness. Experimental identification of  $f_a$  is more common due to the non linear characteristics involved. For pipes that undergo changes in pipe diameters, in general, flow type or over-curves, the fluidic resistance denoted  $R$  may be related to the pressure drop as:

$$\sqrt{\Delta P} = RQ. \quad (3)$$

For a tube, the fluidic resistance is given by:

$$R = \sqrt{f_a \frac{L\rho}{2DA^2}}. \quad (4)$$

For a nozzle (Fig 1), the fluidic resistance is given by:

$$R = \sqrt{\frac{\rho}{2C_dA}} \quad (5)$$

where the unitless  $C_d$  is the discharge coefficient. The discharge coefficient of an orifice atomizer is governed in part by the pressure losses undergoing at the flow passages of the nozzle and also by the extent to which the liquid flows through the final discharge orifice diameter denoted  $d$  [ $mm$ ] [14].

In addition, the pressure drop and the outlet orifice diameter affects the size of the droplets in the spray [15]. In Figure 2, it can be observed the volume median diameter of the drops denoted  $VMD$  [ $\mu m$ ] influenced by the diameter of the discharge orifice  $d$ .

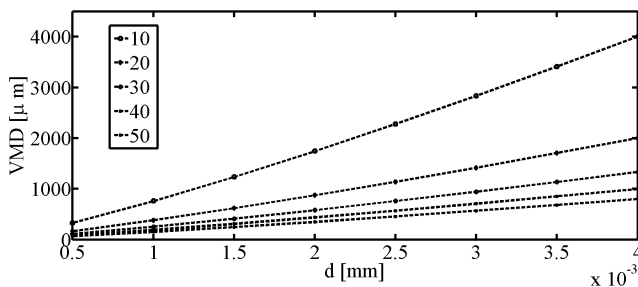


Figure 2. Relationship between the diameter of the nozzle orifice  $d$  and the mean diameter of the drops, which were simulated for different values of exit velocity  $V_i$  in [ $m/s$ ] for a full cone nozzle (figure extracted from [15]).

The output velocity of the mixture  $V_i$  [ $m/s$ ] is also shown in Fig. 2. This velocity depends on the pressure and flow of the liquid in the nozzle.

### III. THEORETICAL BACKGROUND

In this section the theoretical background of the parameterized input-output model and the point-wise Thévenin's equivalent are presented.

#### A. A Parameterized Input-Output Model

In many design problems there is a set of parameters denoted by a vector  $\mathbf{p}$ , whose influence on the output is important to know. The parameters of interest in this work are the orifice diameter, drop pressure, and the Thévenin's equivalent fluidic resistance.

For easy reference, in this section it is describe the main results used in this work following [16]. Consider a linear, parameterized, input-output in matrix form:

$$\begin{aligned} A(\mathbf{p})\mathbf{x} &= B\mathbf{u} \\ \mathbf{y} &= C(\mathbf{p})\mathbf{x} + D\mathbf{u} \end{aligned} \quad (6)$$

where  $A, B, C, D$  are matrices of size  $n \times n, n \times r, n \times m$  and  $m \times r$ , respectively and  $\mathbf{y}, \mathbf{u}, \mathbf{x}$  and  $\mathbf{p}$  denotes the  $m$ -output vector,  $r$ -input vector,  $n$ -state vector and  $\ell$ -parameter vector, respectively. With  $\mathbf{z} \triangleq (\mathbf{x} \ \mathbf{y})'$ , (6) can be written as:

$$T(\mathbf{p}) \mathbf{z} = \begin{pmatrix} B \\ -D \end{pmatrix} \mathbf{u} \text{ where } T(\mathbf{p}) \triangleq \begin{pmatrix} A(\mathbf{p}) & 0 \\ C(\mathbf{p}) & -I \end{pmatrix}.$$

Let

$$T_{ij}(\mathbf{p}) \triangleq \begin{pmatrix} A(\mathbf{p}) & b_j \\ c_i(\mathbf{p}) & -d_{ij} \end{pmatrix}, i = 1, \dots, m, j = 1, \dots, r \quad (7)$$

with  $c_i(\mathbf{p}), i = 1, \dots, m$  being the  $i$ -th row of  $C(\mathbf{p})$ ,  $b_j, j = 1, \dots, r$  the  $j$ -th column of  $B$ ,  $d_{ij}$  the  $ij$ -th element of  $D$ , and

$$\beta_{ij}(\mathbf{p}) \triangleq |T_{ij}(\mathbf{p})|, \alpha(\mathbf{p}) \triangleq |T(\mathbf{p})|. \quad (8)$$

For the model (6), the outputs can be determined in terms of inputs and parameters. This is established below using the results given in [17] and [18]. The following assumptions are needed to establish the results.

*Assumption 1:* The parameter  $\mathbf{p}$  appears affinely in  $A(\mathbf{p})$  and  $C(\mathbf{p})$ :

$$\begin{aligned} A(\mathbf{p}) &= A_0 + p_1 A_1 + \dots + p_\ell A_\ell \\ C(\mathbf{p}) &= C_0 + p_1 C_1 + \dots + p_\ell C_\ell. \end{aligned} \quad (9)$$

*Assumption 2:*

$$|T(\mathbf{p})| \neq 0, \mathbf{p} \in \mathcal{P}. \quad (10)$$

*Theorem 1:* For system (6), the output is given by

$$y_i = \sum_{j=1}^r \frac{\beta_{ij}(\mathbf{p})}{\alpha(\mathbf{p})} u_j, \quad i = 1, 2, \dots, m \quad (11)$$

with  $\beta_{ij}(\mathbf{p})$  and  $\alpha(\mathbf{p})$  as already defined.

To describe the solution  $\mathbf{y}$  from (6), one can use a form for the functions  $\alpha(\mathbf{p})$  and  $\beta_{ij}(\mathbf{p})$ .

*Lemma 1:* Let  $A(\mathbf{p}) = A_0 + p_1 A_1 + \dots + p_\ell A_\ell$  with  $\text{rank}(A_i) = r_i, i = 1, 2, \dots, \ell$ . Then  $\alpha(\mathbf{p}) = |A(\mathbf{p})|$  is a multivariate polynomial in  $\mathbf{p}$ , of degree at most  $r_i$  in  $p_i, i = 1, 2, \dots, \ell$ .

Now consider (7) written in polynomial form:

$$T_{ij}(\mathbf{p}) = T_{ij0} + p_1 T_{ij1} + \dots + p_\ell T_{ij\ell}. \quad (12)$$

Applying Lemma 1, one can see that

$$|T_{ij}| = \beta_{ij}(\mathbf{p}) \quad (13)$$

is a multivariate polynomial in  $\mathbf{p}$  of degree at most  $r_{ijk}$  in  $p_k$  where

$$r_{ijk} = \text{rank}(T_{ijk}), \quad (14)$$

with  $i = 1, 2, \dots, m, j = 1, 2, \dots, r, k = 1, 2, \dots, \ell$ .

Then, it can be shown that the determinants of multivariate polynomials in  $\mathbf{p}$  can be written as:

$$|A(\mathbf{p})| = \sum_{i_\ell=0}^{r_\ell} \dots \sum_{i_1=0}^{r_1} \alpha_{i_1 \dots i_\ell} p_1^{i_1} \dots p_\ell^{i_\ell} \quad (15)$$

with  $\text{rank}(A_i) = r_i, i = 1, 2, \dots, \ell$ . In the form of (15), the number of coefficients in  $|A(\mathbf{p})|$  is  $\mu \triangleq \sum_{i=1}^{\ell} (r_i + 1)$ . The following example shows the use of the rank of the matrices  $A_i, i = 1, 2, \dots, m$  to obtain the determinant of a multivariate polynomial in  $\mathbf{p}$ .

*Example 1:* Let

$$A(\mathbf{p}) = \begin{bmatrix} 1 & 2p_1 & 0 \\ p_1 & p_2 & p_1 \\ 3 & p_1 & 3p_2 \end{bmatrix}. \quad (16)$$

As the parameter  $\mathbf{p}$  appears affinely in  $A(\mathbf{p})$ , following (1), one can write

$$A(\mathbf{p}) = \begin{bmatrix} 1 & 0 & 0 \\ 0 & 0 & 0 \\ 3 & 0 & 0 \end{bmatrix} + \begin{bmatrix} 0 & 2 & 0 \\ 1 & 0 & 1 \\ 0 & 1 & 0 \end{bmatrix} p_1 + \begin{bmatrix} 0 & 0 & 0 \\ 0 & 1 & 0 \\ 0 & 0 & 3 \end{bmatrix} p_2.$$

In this example,  $\text{rank}(A_1) = 2, \text{rank}(A_2) = 2$ . Matrix  $A(\mathbf{p})$  is said to be rank 2 with respect to  $p_1$  and  $p_2$ , which yields  $r_1 = 2$  and  $r_2 = 2$ . Thus,

$$|A(\mathbf{p})| = \sum_{i_2=0}^2 \sum_{i_1=0}^2 \alpha_{i_1 i_2} p_1^{i_1} p_2^{i_2}$$

is a polynomial of degree at most 2 in both  $p_1$  and  $p_2$ . Calculating the determinant, it yields

$$|A(\mathbf{p})| = -6p_1^2 p_2 + 5p_1^2 + 3p_2^2.$$

Now consider (7) written in polynomial form:

$$T_{ij}(\mathbf{p}) = T_{ij0} + p_1 T_{ij1} + \dots + p_\ell T_{ij\ell}.$$

Applying Lemma 1, one can see that

$$|T_{ij}| = \beta_{ij}(\mathbf{p})$$

is a multivariate polynomial in  $\mathbf{p}$  of degree at most  $r_{ijk}$  in  $p_k$  where

$$r_{ijk} = \text{rank}(T_{ijk}), i = 1, 2, \dots, m \\ j = 1, 2, \dots, r, k = 1, 2, \dots, \ell$$

and its determinant can be described in a similar manner as in (15).

## B. A Measurement Based Approach To Unknown Systems

The solution (11) suggests that knowledge of the functions  $\alpha(\mathbf{p})$  and  $\beta_{ij}(\mathbf{p})$  are sufficient to determine the behavior of the outputs  $y_i$  as a function of  $\mathbf{p}$  and  $\mathbf{u}$  [18], [19]. The knowledge of  $\alpha(\mathbf{p})$  and  $\beta_{ij}(\mathbf{p})$  reduces to the knowledge of the coefficients of these polynomial functions. In an unknown system (black box, for instance) these coefficients are unknown a priori. However, if one can conduct tests on the system by setting the design parameter  $\mathbf{p}$  and input  $\mathbf{u}$  to various values and measuring the corresponding  $y_i$ , the polynomial functions coefficients can be determined. It is possible illustrate this concept for the special case of a single output  $y_i$  with inputs  $u_1, u_2$  and parameters  $\mathbf{p} = p_1$  for a rank one model from Lemma 1. Here,

$$y_i = \frac{\beta_{i1}(\mathbf{p})}{\alpha(\mathbf{p})} u_1 + \frac{\beta_{i2}(\mathbf{p})}{\alpha(\mathbf{p})} u_2 \quad (17)$$

with

$$\begin{aligned} \beta_{ij}(\mathbf{p}) &= \beta_{ij0} + \beta_{ij1} p_1, j = 1, 2 \\ \alpha(\mathbf{p}) &= \alpha_0 + \alpha_1 p_1. \end{aligned} \quad (18)$$

Assuming  $\alpha_1 \neq 0$ , one may divide both the numerator and denominator of the right hand side of (17) and write a linear algebraic equation to find the unknown coefficients of  $\alpha(\mathbf{p})$  and  $\beta_{ij}(\mathbf{p})$  from measurements as follows.

Set  $u_2 = 0, u_1 = u_1^*$  and measure  $y_i$  for three different sets of values ( $p_1 \triangleq p$ ) to determine the coefficients of  $\alpha(\mathbf{p})$  and  $\beta_{ij}(\mathbf{p}), j = 1, 2$  from the following measurement equation with  $y_i(k)$  denoting the three measurement values and  $p(k)$  the three sets of parameters with  $k = 1, 2, 3$ :

$$\begin{pmatrix} y_i(1) & -u_j(1) & -u_j(1)p(1) \\ y_i(2) & -u_j(2) & -u_j(2)p(2) \\ y_i(3) & -u_j(3) & -u_j(3)p(3) \end{pmatrix} \begin{pmatrix} \alpha_0 \\ \beta_{ij0} \\ \beta_{ij1} \end{pmatrix} = \begin{pmatrix} -y_i(1)p(1) \\ -y_i(2)p(2) \\ -y_i(3)p(3) \end{pmatrix} \quad (19)$$

with  $j = 1, 2$ .

## C. Thévenin's Equivalent From The Input-Output Parameterized Model

Consider a nonlinear source, connected to a linear load named  $R$  as shown in Fig. 3.

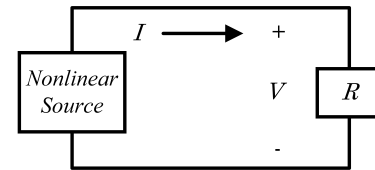


Figure 3. Nonlinear source.

The V-I characteristic of the source is described by:

$$I = f(V) \quad (20)$$

where  $f(V)$  is assumed to be a continuous and differentiable function. The operating point  $(V_o, I_o)$  of the circuit in Fig. 3 can be obtained graphically as shown in Fig. 4.

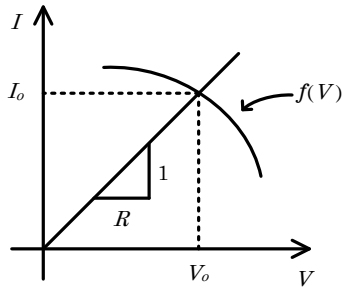


Figure 4. Operating point of a nonlinear circuit.

D. Point-wise Thévenin's Equivalents

Now consider a Thévenin's equivalent of the nonlinear circuit described by the V-I characteristic at the operating point  $(V_o, I_o)$ , which yields the characteristic line  $L$  illustrated in Fig. 5.

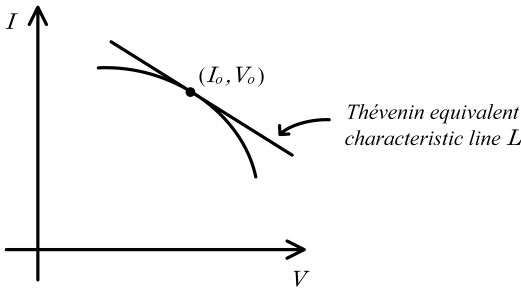


Figure 5. Point-wise Thévenin's equivalent.

The Thévenin's equivalent circuit is represented by the resistance denoted  $R_{th}$  and the voltage denoted  $V_{th}$  connected as shown in Fig. 6. Thus

$$V = V_{th} - IR_{th} \tag{21}$$

and

$$I = -\frac{1}{R_{th}}V + \frac{V_{th}}{R_{th}}. \tag{22}$$

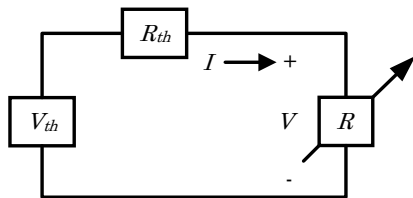


Figure 6. Equivalent circuit.

If (22) is to represent the line shown in Fig. 5, which is tangent to  $f(V)$  at  $(V_o, I_o)$ , one must have:

$$I = MV + C \tag{23}$$

with

$$M = \left. \frac{\partial I}{\partial V} \right|_{(V_o, I_o)} \triangleq M_o$$

$$C = I_o - M_o V_o \triangleq C_o.$$

Comparing (22) and (23) it follows that:

$$-\frac{1}{R_{th}} = M_o \tag{24}$$

$$\frac{V_{th}}{R_{th}} = C_o. \tag{25}$$

Thus, the Thévenin's equivalent of the nonlinear circuit of Fig. 3 at  $(V_o, I_o)$  is given by:

$$R_{th} = -\frac{1}{M_o} \tag{26}$$

$$V_{th} = -\frac{C_o}{M_o}. \tag{27}$$

Note that the above parameters can be determined, if the nonlinear characteristic is known, at any point  $(V_o, I_o)$  and thus a family of point-wise Thévenin's equivalents may be constructed. If the  $I = f(V)$  characteristic is not known, the Thévenin's equivalents may be determined by estimating the parameters of the tangent line  $L$  using a fixed number of measurements.

IV. METHOD

It is known that the flow in a nozzle is a function of the orifice diameter, drop pressure and other hydraulic parameters, which may change with different types of nozzle. Then, it is possible to find a function that relates the orifice diameter and pressure with the flow in a nozzle.

It is assumed that the rank of the matrices appearing in the description of the flow  $Q$  in relation to parameter  $d$  and boom pressure  $\Delta P$  is unity. According to Bhattacharyya and collaborators [18], it is possible to find the rational function:

$$Q = \frac{\beta_0 + \beta_1 d + \beta_2 \Delta P + \beta_3 d \Delta P}{\alpha_0 + \alpha_1 d + \alpha_2 \Delta P + d \Delta P} \tag{28}$$

where  $\beta_0, \beta_1, \beta_2, \beta_3, \alpha_0, \alpha_1$  and  $\alpha_2$  are constants and  $(\alpha_0 + \alpha_1 d + \alpha_2 \Delta P + d \Delta P) \neq 0$ . To obtain these constants, one should take just 7 measurements with different values of  $d$  and  $\Delta P$  and solve the following linear system:

$$\begin{bmatrix} 1 & d(1) & \Delta P(1) & d(1)\Delta P(1) & -Q(1) & -Q(1)d(1) & -Q(1)\Delta P(1) \\ 1 & d(2) & \Delta P(2) & d(2)\Delta P(2) & -Q(2) & -Q(2)d(2) & -Q(2)\Delta P(2) \\ 1 & d(3) & \Delta P(3) & d(3)\Delta P(3) & -Q(3) & -Q(3)d(3) & -Q(3)\Delta P(3) \\ 1 & d(4) & \Delta P(4) & d(4)\Delta P(4) & -Q(4) & -Q(4)d(4) & -Q(4)\Delta P(4) \\ 1 & d(5) & \Delta P(5) & d(5)\Delta P(5) & -Q(5) & -Q(5)d(5) & -Q(5)\Delta P(5) \\ 1 & d(6) & \Delta P(6) & d(6)\Delta P(6) & -Q(6) & -Q(6)d(6) & -Q(6)\Delta P(6) \\ 1 & d(7) & \Delta P(7) & d(7)\Delta P(7) & -Q(7) & -Q(7)d(7) & -Q(7)\Delta P(7) \end{bmatrix} \begin{bmatrix} \beta_0 \\ \beta_1 \\ \beta_2 \\ \beta_3 \\ \alpha_0 \\ \alpha_1 \\ \alpha_2 \end{bmatrix} = \begin{bmatrix} Q(1)d(1)\Delta P(1) \\ Q(2)d(2)\Delta P(2) \\ Q(3)d(3)\Delta P(3) \\ Q(4)d(4)\Delta P(4) \\ Q(5)d(5)\Delta P(5) \\ Q(6)d(6)\Delta P(6) \\ Q(7)d(7)\Delta P(7) \end{bmatrix}. \tag{29}$$

The well known Thévenin's equivalent circuit of a linear circuit is composed of an equivalent impedance and voltage, which for some cases are represented as a resistor and a source of continuous voltage. This equivalent circuit is obtained through Thévenin's Theorem.

*Theorem 1 (Thévenin's Theorem):* The voltage and resistance equivalent of a circuit is given by:

$$V_{th} = V_{oc} \quad (30)$$

$$R_{th} = \frac{V_{oc}}{I_{sc}} \quad (31)$$

where  $I_{sc}$  is the short-circuit current and  $V_{oc}$  the open circuit voltage [20]–[23].

The Thévenin's equivalent circuit can be represented by Fig 6. In Fig. 6, the voltage and current are described by:

$$I = \frac{V_{th}}{R_{th} + R} \quad (32)$$

$$V = RI = -R_{th}I + V_{th}. \quad (33)$$

Let  $y(1)$  and  $y(2)$  denote current measurements taken with the values of the load  $R$  denoted  $R(1)$  and  $R(2)$ , respectively. According to Bhattacharyya and collaborators [18] and Mohsenizadeh and collaborators [19], the Thévenin's equivalent can also be obtained by solving the linear equation system, in terms of  $\alpha_0$  and  $\beta_0$ :

$$\begin{pmatrix} y(1) & -1 \\ y(2) & -1 \end{pmatrix} \begin{pmatrix} \alpha_0 \\ \beta_0 \end{pmatrix} = \begin{pmatrix} -y(1)R(1) \\ -y(2)R(2) \end{pmatrix} \quad (34)$$

where  $\alpha_0$  and  $\beta_0$  are given by:

$$\alpha_0 = R_{th} \quad (35)$$

$$\beta_0 = V_{th}. \quad (36)$$

If one is considering a linear characteristic then is possible to write:

$$V_{oc} = V_{th} \quad (37)$$

$$I_{sc} = \frac{V_{th}}{R_{th}}. \quad (38)$$

One can consider, as a further step, the electric analog already described in Section I, then  $V = \sqrt{\Delta P}$  e  $V_{th} = \sqrt{\Delta P_{th}}$ . Now, let  $y(1)$  e  $y(2)$  be measures of flow in the boom with the nozzles of interest, and let  $R(1)$  and  $R(2)$  correspond to the equivalent fluidic resistance of the nozzles of the boom of interest, thus:

$$\begin{pmatrix} Q(1) & -1 \\ Q(2) & -1 \end{pmatrix} \begin{pmatrix} \alpha_0 \\ \beta_0 \end{pmatrix} = \begin{pmatrix} -\sqrt{\Delta P(1)} \\ -\sqrt{\Delta P(2)} \end{pmatrix} \quad (39)$$

where  $\alpha_0$  e  $\beta_0$  are given by:

$$\alpha_0 = R_{th} \quad (40)$$

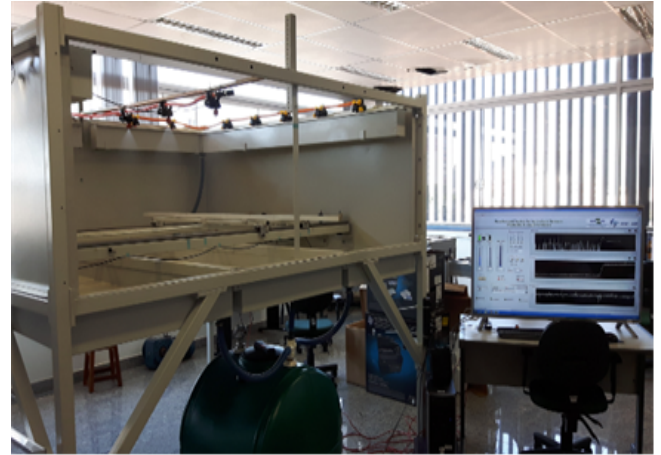
$$\beta_0 = \Delta P_{th}. \quad (41)$$

where  $R_{th}$  and  $\Delta P_{th}$  are the internal loss and pressure equivalent, respectively. As the behavior of pressure and flow is non-linear, then there will be more than one possible representation

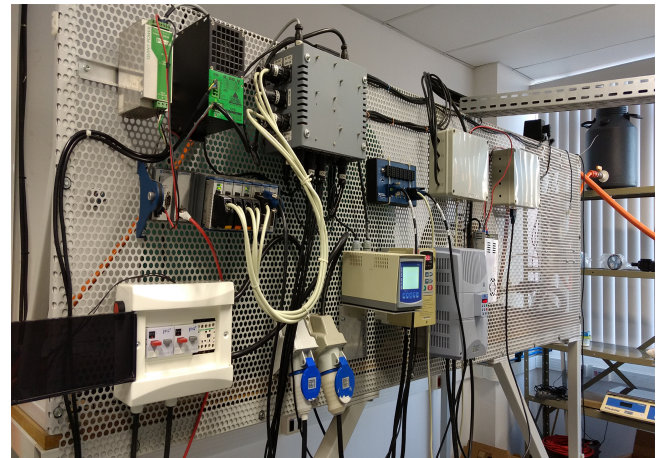
of the Thévenin's equivalent. If the measurements are taken as close as possible to each other, it is then said that a point-wise Thévenin's equivalent is obtained.

## V. EXPERIMENTAL VALIDATION

The Agricultural Sprayer Development System (SDPA) used to obtain experimental results is located at the Laboratory for Precision Agricultural inputs Applications of the Embrapa Instrumentation (Figs. 7 and 8) in São Carlos, SP, Brazil [24]–[28]. The goal is to describe the flow in function of the orifice  $d$  and pressure drop  $\Delta P$  and to obtain the linear pressure and fluidic resistance equivalent by selecting a boom with nozzles of interest using regular measurements.



(a)



(b)

Figure 7. Detail in photos of the SDPA containing: a) spray booms of agricultural pesticides and monitoring platform, b) control panel and data acquisition devices.

The results were separated into two different experiments. The first experiment was performed to find the coefficients of (28), which are related to the orifice diameter and pressure in the nozzle. The second experiment was carried out to obtain the Thévenin's equivalent, where the goal was to obtain the linear pressure and the fluidic resistance equivalent by selecting a boom with nozzles of interest and using regular measurements, which is possible by solving (34).

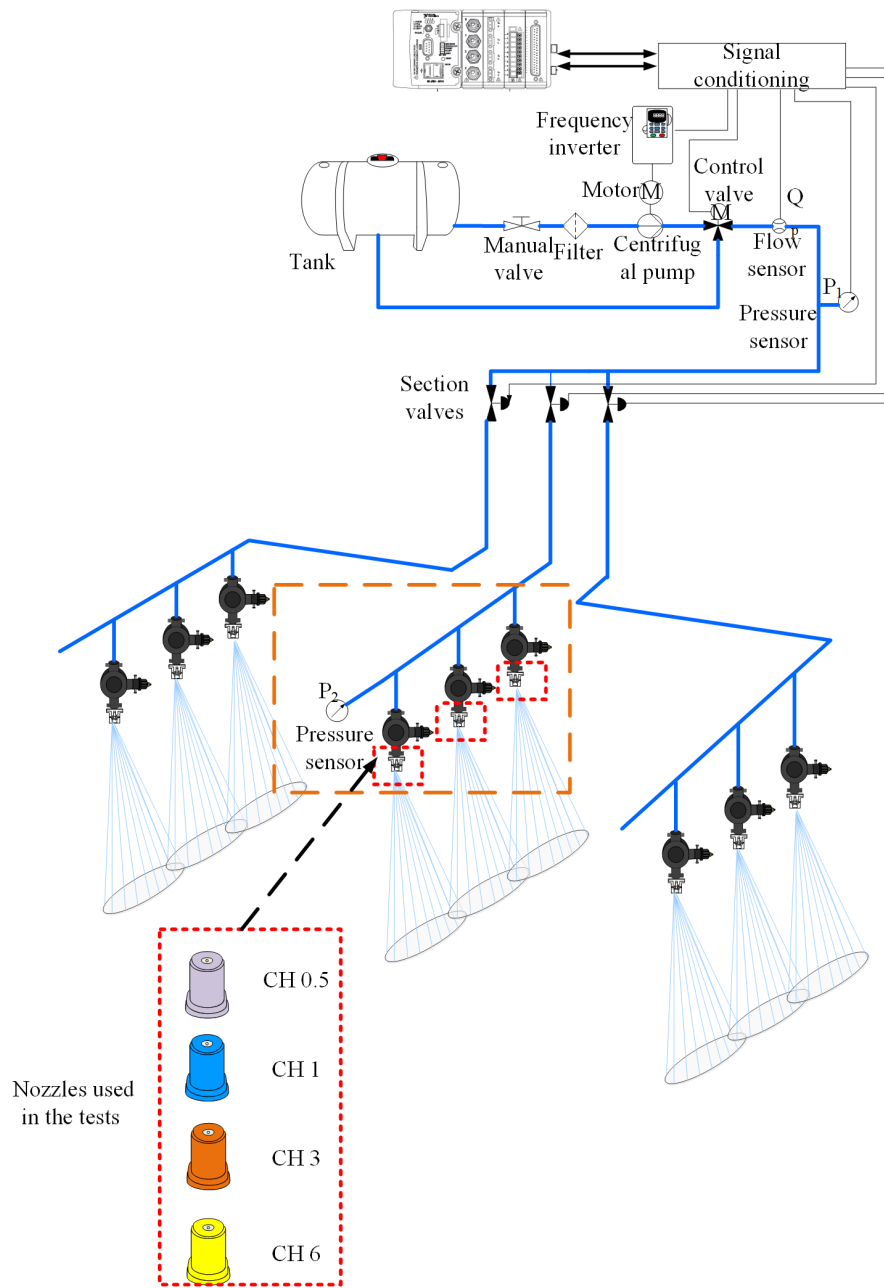


Figure 8. Hydraulic and electrical configuration of the SDPA for testing and estimation of the fluidic resistance of the nozzles.

A. Nozzle Flow Validation

To validate (28), which relates the flow to the orifices diameters, the nozzles were used. The datasheet of a nozzle MAG CH, produced by MAGNOJET®, was used. Then it was possible to find the values of pressure and flow for each nozzle. The orifices diameters were measured using a pachymeter. The

7 points shown in Table I were selected, which cover the entire producer table, and were used to solve the linear system (29). The evaluated matrix is shown in (42) and the coefficients solution are shown in Table II. With the solution of (29), it was possible to generate the surface shown in Fig. 9.

$$\begin{bmatrix} 1.00 & 0.50 & 3.40 & 1.70 & -0.56 & -0.28 & -1.90 \\ 1.00 & 1.50 & 3.40 & 5.10 & -1.50 & -2.25 & -5.10 \\ 1.00 & 2.00 & 3.40 & 6.80 & -2.40 & -4.80 & -8.16 \\ 1.00 & 0.50 & 10.40 & 5.20 & -0.94 & -0.47 & -9.78 \\ 1.00 & 1.50 & 10.40 & 15.60 & -2.55 & -3.83 & -26.50 \\ 1.00 & 2.00 & 10.40 & 20.80 & -4.08 & -8.16 & -42.40 \\ 1.00 & 1.50 & 7.60 & 11.40 & -2.20 & -3.30 & -16.70 \end{bmatrix} \begin{bmatrix} \beta_0 \\ \beta_1 \\ \beta_2 \\ \beta_3 \\ \alpha_0 \\ \alpha_1 \\ \alpha_2 \end{bmatrix} = \begin{bmatrix} 0.95 \\ 7.65 \\ 16.30 \\ 4.89 \\ 39.80 \\ 84.90 \\ 25.10 \end{bmatrix} . \tag{42}$$

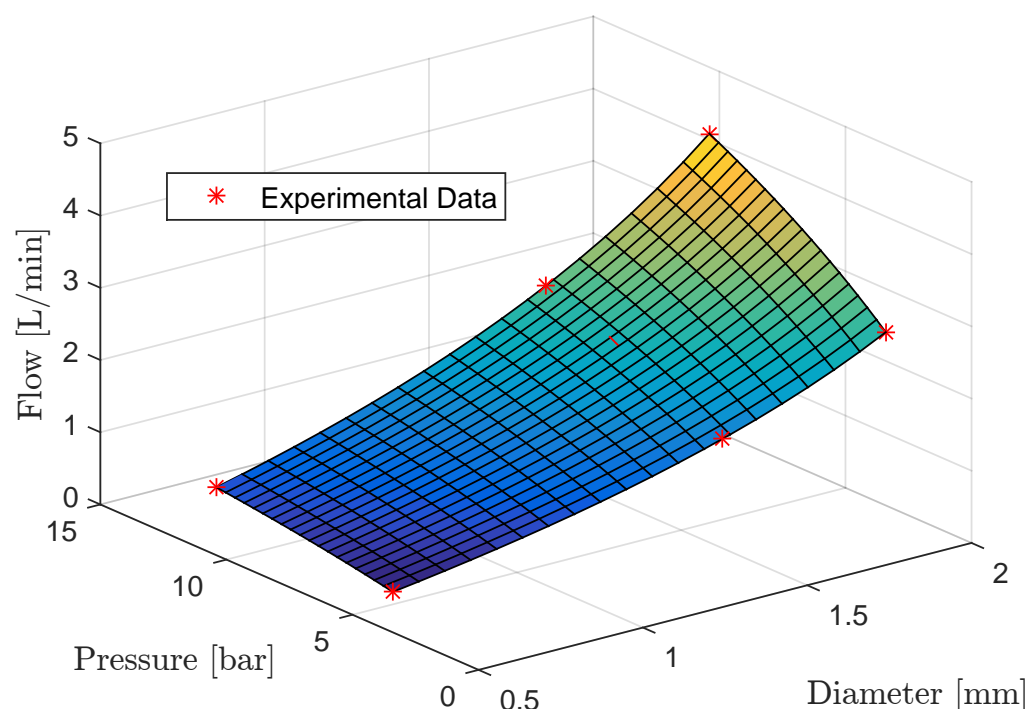


Figure 9. Surface relating the orifice diameter  $d$  and the pressure with the output flow for the full cone nozzle.

TABLE I. SELECTED MEASUREMENTS FROM THE MAGNOJET PRODUCER DATASHEET.

Nozzle	Pressure [bar]	Q [L/min]	d [mm]
CH05	3.40	0.56	0.50
CH3	3.40	1.50	1.50
CH6	3.40	2.40	2.00
CH05	10.40	0.94	0.50
CH3	10.40	2.55	1.50
CH6	10.40	4.08	2.00
CH3	7.60	2.20	1.50

TABLE II. COEFFICIENTS of (29) obtained.

$\beta_0$	$\beta_1$	$\beta_2$	$\beta_3$
-9.81	-11.61	-3.81	-5.99
$\alpha_0$	$\alpha_1$	$\alpha_2$	
-67.54	18.65	-3.74	

TABLE III. PREDICTED FLOW AND THE CATALOG FLOW TO CH1 NOZZLE USING THE SURFACE

Pressure [bar]	$d$ [mm]	Predicted flow [L/min]	Catalog Flow [L/min]	Relative error [%]
3.40	1.00	0.94	1.00	5.90
4.80	1.00	1.10	1.20	8.00
6.20	1.00	1.25	1.33	6.17
7.60	1.00	1.38	1.47	6.39
9.00	1.00	1.49	1.63	8.54
10.40	1.00	1.60	1.74	8.39

Using Fig. 9 it is possible now to predict the flow of the nozzle given the diameter of the orifice and the pressure in the

nozzle, what can help in the design of the nozzle. In Table III, the results of the prediction using the nozzle CH1 are shown.

### B. Thévenin's Equivalent Validation

To obtain the hydraulic Thévenin equivalent, according to the proposed methodology, only two different fluidic resistances are required. However, it is necessary that when the fluidic resistance changes, a significant variation of pressure and flow occurs at the point of interest. Otherwise, if any of these measures are kept constant, a solution does not exist.

A pressure variation, in relation to the pump pressure, of approximately 0.1 bar at the point of interest was considered significant because of the inherent noise of the spray sensors. The objective is to extract the Thévenin's equivalent of the central sprayer boom, which is also shown in Fig. 8. All nozzles of the central sprayer boom are of type CH05.

1) *Measurements set-up:* Firstly, the central sprayer boom had 3 spray nozzles type CH05. The pump pressure was set to 3.5 bar and the corresponding pressure at the center boom spray nozzles was found to be about 3.48 bar. Then, only one of the 3 nozzles was changed to type CH3. The pressure in the spray nozzles rose to 3.47 bar and was therefore again considered as noise. Another attempt was made by replacing the same nozzle by a nozzle type CH6 (which allowed the largest flow in this line). The pressure at the nozzles rose to 3.46 and was again considered as noise. Two nozzle were then replaced by CH3 type nozzles and the pressure at the spray nozzles was found to be 3.44 bar, again considered to be noise. In this way, all the nozzles of the central bar were changed to type CH3 and the pressure was equal to 3.39 bar. This pressure drop was then considered as significant and thus concluding that it was necessary to change all the nozzles of the boom to take the measurements.

To extract the Thévenin's equivalent, only two different nozzles were required. To validate the Thévenin's equivalent obtained, a third different nozzle with an intermediate fluidic resistance between the other two nozzles was used to extract the equivalent. The resulting data are shown in Table IV.

TABLE IV. DATA OBTAINED FOR DIFFERENT FULL CONE NOZZLES

Nozzles	Pressure [bar]	Flow [L/min]
CH05	3.40	0.53
CH3	3.35	1.42
CH6	3.29	2.23

Using (39), the following equivalent was obtained:

$$\Delta P_{th} = 1.85 \text{ [bar]}$$

$$R_{th} = 0.02 \text{ [bar} \cdot \text{min} \cdot \text{L}^{-1}\text{]}.$$

Thus, this equivalent was used to estimate the flow of arbitrary pressure values. The result is shown in Fig. 10. The error of estimated flow was around 2.15%.

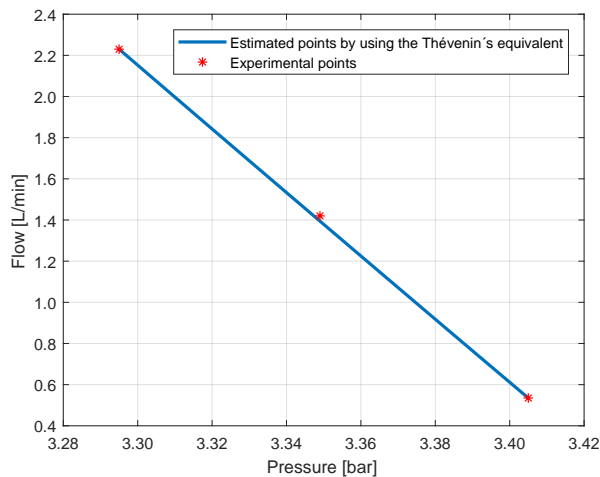


Figure 10. Thévenin's equivalent for full cone nozzles.

## VI. CONCLUSION

In this paper, a measurement-based approach was used to emulate the behavior of a sensor to allow the control quality analyses of direct injection sprayers. With few measurement, a flow function of a full cone nozzle relating the nozzle internal diameter and pressure were estimated. In addition, the fluidic resistance equivalent of a piping system was obtained.

The results presented showed that using the proposed method, one can be able to find the relationship among the orifice diameter of the nozzles, pressure and the flow for an adjusted operation using a graphical surface inspection. In addition, from the point-wise fluidic resistance the conditions necessary for the correct operation of each nozzle can be defined.

The experimental results obtained were satisfactory and the extension of this work includes the hardware implementation of the sensor and the application of the measurement-based approach to analyze the control quality of spray droplets in agriculture.

## ACKNOWLEDGMENT

This work was supported by the Brazilian Agricultural Research Corporation - Embrapa (grant numbers MP2 - 02.11.07.025.00.00, MP1 - 01.14.09.001.05.05); the National Counsel of Technological and Scientific Development - CNPq (grant number 306.477/2013-0). The authors also thank the MAGNOJET<sup>®</sup> by the availability of the nozzles for validation of the developed method.

## REFERENCES

- [1] R. F. Q. Magossi, E. A. G. Peñaloza, S. P. Battacharya, V. A. Oliveira, and P. E. Cruvinel, "Using the measurement-based approach to emulate the behavior of a sensor for internal hydraulic pressure drop measurements of sprayers in the agricultural industry," in *ALLSENSORS 2017: The Second International Conference on Advances in Sensors, Actuators, Metering and Sensing*. IARIA, Mar. 2017, pp. 10–15.
- [2] R. Mulley, *Flow of industrial fluids: theory and equations*. CRC Press, 2004.
- [3] L. E. Bode and S. M. Bretthauer, "Agricultural chemical application technology: a remarkable past and an amazing future," *Transactions of the ASAE*, vol. 51, no. 2, p. 391, 2008.
- [4] P. Chueca, C. Garcera, E. Molto, and A. Gutierrez, "Development of a sensor-controlled sprayer for applying low-volume bait treatments," *Crop Protection*, vol. 27, no. 10, pp. 1373–1379, 2008.
- [5] S. Han, L. L. Hendrickson, B. Ni, and Q. Zhang, "Modification and testing of a commercial sprayer with pwm solenoids for precision spraying," *Applied Engineering in Agriculture*, vol. 5, no. 17, pp. 591–594, 2001.
- [6] F. H. R. Baio and U. R. Antuniassi, "Sistemas de controle eletrônico e navegação para pulverizadores (electronic control and navigation systems for sprayers)," in *Tecnologia de Aplicação para Culturas Anuais (Application Technology for Annual Crops)*, U. R. Antuniassi and W. Boller, Eds. Passo Fundo: Aldeia Norte, 2011.
- [7] P. E. Cruvinel, D. Karam, and M. G. Beraldo, "Method for the precision application of herbicides in the controlling of weed species into a culture of maize," in *VII Simpósio Internacional de Tecnologia de Aplicação (International Symposium on Application Technology)*. Uberlândia, MG: SINTAG, 2015.
- [8] B. L. Steward and D. S. Humburg, "Modeling the raven scs-700 chemical injection system with carrier control with sprayer simulation," *Transactions of the ASAE*, vol. 43, no. 2, pp. 231–245, 2000.
- [9] A. Akers, M. Gassman, and R. Smith, *Hydraulic Power System Analysis*. Broken Sound Parkway: CRC Press, 2006.
- [10] J. Zhang, Y. Ju, S. Zhou, and C. Zhou, "Air-pasty propellant pressure drop and heat transfer through round pipe," in *2008 Asia Simulation Conference - 7th International Conference on System Simulation and Scientific Computing*, Oct. 2008, pp. 1282–1285.
- [11] Y. Suzumura and P. E. Cruvinel, "Análise de qualidade da eficiência da pulverização agrícola com processamento de imagem e rede neural (quality analysis of crop spray efficiency with image processing and neural network)," *Sinergia*, vol. 6, no. 2, pp. 129–137, 2005.
- [12] R. A. Kohl, "Drop size distribution from medium-sized agricultural sprinklers," *Transaction of the ASAE*, vol. 17, no. 4, pp. 690 – 693, 1974.
- [13] P. A. Tipler and G. Mosca, *Physics for Scientists and Engineers*, 6th ed. New York: W. H. Freeman, 2007.
- [14] A. Lefebvre, *Atomization and Sprays*, ser. Combustion, Hemisphere Publishing Corporation. Boca Raton, FL, USA: Taylor & Francis, 1988.
- [15] E. A. G. Peñaloza, H. V. Mercaldi, V. A. Oliveira, and P. E. Cruvinel, "An advanced model based on analytical and computational procedures for the evaluation of spraying processes in agriculture," in *2016 IEEE Tenth International Conference on Semantic Computing (ICSC)*. IEEE, Feb. 2016, pp. 432–436.
- [16] D. N. Mohsenzadeh, V. A. Oliveira, L. H. Keel, and S. P. Bhattacharyya, "Extremal results for algebraic linear interval systems," in *Optimization and Its Applications in Control and Data Sciences*, B. Goldengorin, Ed. Switzerland: Springer International Publishing, 2016, pp. 341–351.

- [17] V. A. Oliveira, K. R. Felizardo, and S. P. Bhattacharyya, "A model-free measurement based approach to circuit analysis and synthesis based on linear interval systems," in *IEEE International Symposium on Industrial Electronics (ISIE)*, June 2015, pp. 1–6.
- [18] S. P. Bhattacharyya, L. H. Keel, and D. Mohsenizadeh, *Linear Systems: A Measurement Based Approach*, ser. Springer Briefs in Applied Sciences and Technology. Springer, 2013.
- [19] N. Mohsenizadeh, H. Nounou, M. Nounou, A. Datta, and S. P. Bhattacharyya, "Linear circuits: a measurement-based approach," *International Journal of Circuit Theory and Applications*, vol. 43, no. 2, pp. 205–232, 2015.
- [20] L. Thévenin, "Extension de la loi d'ohm aux circuits électromoteurs complexes (Extension of Ohm's law to complex electromotive circuits)," *Annales Télégraphiques*, vol. 10, no. 222-224, 1883.
- [21] L. Thévenin, "Sur un nouveau théorème d'électricité dynamique (On a new theorem of dynamic electricity)," *C. R. des Séances de l'Académie des Sciences*, vol. 97, no. 159-161, 1883.
- [22] J. Brittain, "Thevenin's theorem," *Spectrum, IEEE*, vol. 27, no. 3, pp. 42–, 1990.
- [23] D. Johnson, "Origins of the equivalent circuit concept: the current-source equivalent," *Proceedings of the IEEE*, vol. 91, no. 5, pp. 817–821, 2003.
- [24] P. E. Cruvinel, V. A. Oliveira, H. V. Mercaldi, E. A. G. Peñaloza, and K. R. Felizardo, "An advanced sensors-based platform for the development of agricultural sprayers," in *Sensors and Applications in Measuring and Automation Control Systems*. IFSA, Dec. 2016, pp. 181–204.
- [25] P. E. Cruvinel, V. A. Oliveira, K. R. Felizardo, and H. V. Mercaldi, "Bancada automatizada para ensaios e desenvolvimento de pulverizadores de agrotóxicos, aplicadores de fertilizantes líquidos e maturadores em culturas agrícolas sob manejo baseado em agricultura de precisão (Automated bench for testing and development of pesticide sprays, liquid fertilizer applicators and ripeners in agricultural crops under precision agriculture based management)," in *Agricultura de Precisão: um Novo Olhar*. São Carlos, SP: Embrapa Instrumentação, 2011, pp. 96–100.
- [26] H. V. Mercaldi, C. H. Fujiwara, E. A. G. Peñaloza, V. A. Oliveira, and P. E. Cruvinel, "An intelligent and customized electrical conductivity sensor to evaluate the response time of a direct injection system," in *SENSORDEVICES 2015 The Sixth International Conference on Sensor Device Technologies and Applications*. IARIA, 2015, pp. 19 – 24.
- [27] K. R. Felizardo, H. V. Mercaldi, P. E. Cruvinel, V. A. Oliveira, and B. L. Steward, "Modeling and model validation of a chemical injection sprayer system," *Applied Engineering in Agriculture*, vol. 32, no. 3, pp. 285–297, 2016.
- [28] E. A. G. Peñaloza, P. E. Cruvinel, V. A. Oliveira, and A. G. F. Costa, "A model approach to infer the quality in agricultural sprayers supported by knowledge bases and experimental measurements," *International Journal of Semantic Computing*, vol. 11, no. 03, pp. 279–292, 2017.